A combined crossed beam and *ab initio* investigation on the reaction of carbon species with C_4H_6 isomers. II. The dimethylacetylene molecule, $H_3CCCCH_3(X^1A_{1g})$

L. C. L. Huang, H. Y. Lee,[a] A. M. Mebel, S. H. Lin,[a] Y. T. Lee,[a] and R. I. Kaiser[b]
Institute of Atomic and Molecular Sciences, 1, Section 4, Roosevelt Road, 107 Taipei, Taiwan, Republic of China

(Received 29 March 2000; accepted 11 July 2000)

The reaction of ground state carbon atoms, $C(^3P_j)$, with dimethylacetylene, H_3CCCCH_3, was studied at three collision energies between 21.2 and 36.9 $kJmol^{-1}$ employing the crossed molecular beam approach. Our experiments were combined with *ab initio* and RRKM calculations. It is found that the reaction is barrierless via a loose, early transition state located at the centrifugal barrier following indirect scattering dynamics through a complex. $C(^3P_j)$ attacks the π system of the dimethylacetylene molecule to form a dimethylcyclopropenylidene intermediate either in one step via an addition to C1 and C2 of the acetylenic bond or through an addition to only one carbon atom to give a short-lived cis/trans dimethylpropenediylidene intermediates followed by ring closure. The cyclic intermediate ring opens to a linear dimethylpropargylene radical which rotates almost parallel to the total angular momentum vector **J**. This complex fragments to atomic hydrogen and a linear 1-methylbutatrienyl radical, $H_2CCCCCH_3(X^2A'')$, via a tight exit transition state located about 18 $kJmol^{-1}$ above the separated products. The experimentally determined exothermicity of 190 ± 25 $kJmol^{-1}$ is in strong agreement with our calculated data of 180 ± 10 $kJmol^{-1}$. The explicit verification of the carbon versus hydrogen exchange pathway together with the first identification of the $H_2CCCCCH_3$ radical represents a third pathway to form chain C_5H_5 radicals in the reactions of $C(^3P_j)$ with C_4H_6 isomers under single collision conditions. Previous experiments of atomic carbon with the 1,3-butadiene isomer verified the formation of 1- and 3-vinylpropargyl radicals, $HCCCHC_2H_3(X^2A'')$, and $H_2CCCC_2H_3(X^2A'')$, respectively. In high-density environments such as combustion flames and circumstellar envelopes of carbon stars, these linear isomers can undergo collision-induced ring closure(s) and/or H atom migration(s) which can lead to the cyclopentadienyl radical. The latter is thought to be a crucial reactive intermediate in soot formation and possibly in the production of polycyclic aromatic hydrocarbon molecules in outflow of carbon stars. Likewise, a H atom catalyzed isomerization can interconvert the 3-vinylpropargyl and the 1-methylbutatrienyl radical. © *2000 American Institute of Physics.* [S0021-9606(00)00438-4]

I. INTRODUCTION

Investigating the production routes to distinct C_5H_5 isomers is an important means to test chemical models on the formation of polycyclic aromatic hydrocarbons (PAHs) in oxygen-deficient hydrocarbon flames[1] and carbon-rich outflows of late-type, carbon-rich stars. In these outflows, PAH molecules are considered as the condensation nuclei to form larger carbon-rich grain material which itself can be redistributed in the interstellar medium. A postulated reaction pathway to the most simplest PAH, naphthalene, is thought to proceed either via cyclopentadienyl,[2] C_5H_5, or phenyl radicals, C_6H_5, which react with (substituted) acetylene precursors.[3] Both models underline the crucial importance of a stepwise ring extension via five- or six-membered cyclic structures.[4] However, even though the synthetic route via the simple pentacycle C_5H_5 might resemble the key step to build up PAHs, mechanistical studies investigating the formation of cyclopentadienyl radicals are sparse. Therefore, we setup a systematic research program addressing this unsolved mystery. Recent crossed molecular beam experiments of atomic carbon in its ^3P_j electronic ground state with alkynes and olefines demonstrated the existence of a $C(^3P_j)$ versus H exchange channel. Therefore, a formation of C_5H_5 and atomic hydrogen might proceed via C_5H_6 intermediates which are formed by reaction of $C(^3P_j)$ with C_4H_6 isomers 1,3-butadiene, dimethylacetylene, 1,2-butadiene, or ethylacetylene.[5] In the first article of this series, we unraveled the chemical reaction dynamics and triply differential cross sections to form 1- and 3-vinylpropargyl radicals, $HCCCHC_2H_3(X^2A'')$, and $H_2CCCC_2H_3(X^2A'')$, via the reaction of carbon atoms with 1,3-butadiene.[6] In this article, we extend this investigation to the dimethylacetylene isomer, CH_3CCCH_3.

II. EXPERIMENTAL SETUP

The experiments were performed employing the 35″ crossed molecular beams machine described in Ref. 7 in de-

[a]Also at Department of Chemistry, National Taiwan University, Taipei, 107, Taiwan, Republic of China.
[b]Author to whom correspondence should be addressed. Also with Department of Physics, National Taiwan University, Taipei, 107; and Department of Physics, Technical University Chemnitz 09107 Chemnitz, Germany. Electronic mail: kaiser@po.iams.sinica.edu.tw

TABLE I. Experimental beam conditions and 1σ errors averaged over the experimental time: peak velocity v_p, speed ratio S (Ref. 24) peak collision energy, E_{coll}, center-of-mass angle, $\theta_{C.M.}$, composition of the carbon beam, and flux factor $f_v = n(C)*n(H_2CCCH_2)*v_r$ in relative units, with the number density of the ith reactant n_i and the relative velocity v_r.

Beam	v_p (ms^{-1})	S	E_{coll} (kJmol^{-1})	$\theta_{C.M.}$	C_1:C_2:C_3	f_v
$C(^3P_j)$	1930±40	7.1±0.2	21.2±0.9	61.0±0.2	1:0.2:0.6	1.0
$C(^3P_j)$	2310±50	6.6±0.2	29.1±1.2	56.5±0.2	1:0.3:0.7	1.3±0.2
$C(^3P_j)$	2630±50	4.4±0.2	36.9±1.3	53.0±1.0	1:0.2:0.7	1.6±0.3
C_4H_6	775±10	9.1±0.2	⋯	⋯	⋯	⋯

tail. A pulsed supersonic carbon beam was generated via laser ablation of graphite at 266 nm.[8] The 30 Hz, 35–40 mJ output of a Spectra Physics GCR-270-30 Nd:YAG laser was focused onto a rotating carbon rod, and the ablated species were seeded into a pulse of neat helium gas at 4 atm backing pressure. A four-slot chopper wheel mounted after the ablation zone selected a 9.0 μs segment of the seeded carbon beam. Table I compiles the experimental beam conditions. The carbon beam and a pulsed dimethylacetylene beam at 450±10 torr backing pressure passed through skimmers and crossed at 90° in the interaction region of the scattering chamber. Reactively scattered products were detected in the plane defined by two beams using a rotable detector consisting of a Brink-type electron-impact ionizer,[9] quadrupole mass filter, and a Daly ion detector at laboratory angles between 3.0° and 72.0° with respect to the primary beam. The velocity distribution of the products was recorded using the time-of-flight (TOF) technique accumulating between 30 and 120 min at each angle. Information on the chemical reaction dynamics was gained by fitting the TOF spectra and the product angular distribution in the laboratory frame (LAB) using a forward-convolution routine.[10] This procedure assumes an angular flux distribution $T(\theta)$ and the translational energy flux distribution $P(E_T)$ in the center-of-mass system (C.M.). Laboratory TOF spectra and the laboratory angular distributions were then calculated from these $T(\theta)$ and $P(E_T)$ averaged over the apparatus and beam functions. Best TOF and laboratory angular distributions were archived by refining adjustable $T(\theta)$ and $P(E_T)$ parameters. The final outcome is the generation of a product flux contour map which reports the differential cross section, $I(\theta,u) \sim P(u)*T(\theta)$, as the intensity as a function of angle θ and product center-of-mass velocity u.

III. ELECTRONIC STRUCTURE AND RRKM CALCULATIONS

The geometries of the reactants, products, intermediates, and transition states for the $C(^3P_j)+H_3CCCC_3H$ reaction were optimized using the hybrid density functional B3LYP method[11] with the 6-311G(d,p) basis set.[12] Vibrational frequencies, calculated at the B3LYP/6-311G(d,p) level, were used for characterization of stationary points as minima (zero imaginary frequencies) or transition states (one imaginary frequency), for zero-point energy (ZPE) corrections and for Rice–Ramsperger–Kassel–Marcus (RRKM) calculations. The energies were refined using the G2M(RCC,MP2) method[13] which gives an approximation for RCCSD(T)/6-311+G($3df,2p$). This approach was demonstrated to provide chemical accuracy for the energetics of local minima and transition states.[13] The GAUSSIAN 98[14] and MOLPRO-98[15] programs were employed for the potential energy surface computations. In this article, we present only those results necessary to understand our experimental data. More detailed information concerning the structure of intermediates and transition states will be given in a forthcoming publication.

We used the RRKM theory[16] for computations of rate constants of individual reaction steps. Rate constant $k(E)$ at a collision energy E for a unimolecular reaction $A^* \rightarrow A^{\#} \rightarrow P$ can be expressed as

$$k(E) = \frac{\sigma}{h} \frac{W^{\#}(E-E^{\#})}{\rho(E)},$$

where σ is a symmetry factor, $W^{\#}(E-E^{\#})$ denotes the total number of states for the transition state (activated complex) $A^{\#}$ with a barrier $E^{\#}$, $\rho(E)$ represents the density of states of the energized reactant molecule A^*, and P is the product or products. The saddle point method was applied to evaluate $\rho(E)$ and $W(E)$.[16]

IV. RESULTS

A. Reactive scattering signal

Similar to the reaction of $C(^3P_j)$ with 1,3-butadiene reactive scattering signal was observed at mass to charge ratios $m/e=65$ ($C_5H_5^+$) to 60 (C_5^+), cf. Figs. 1–6. Since all TOF spectra could be fit with the same $T(\theta)$ and $P(E_T)$, the signal at lower m/e ratios must originate in the cracking of the $C_5H_5^+$ parent ion in the ionizer. Therefore, data were taken at $m/e=65$ because of the highest signal-to-noise ratio at this mass-to-charge ratio. We did not detect any signal at $m/e=66$ (C_5H_6); therefore, the radiative association channel to the C_5H_6 adduct is closed. In addition, we checked the methyl loss channel to form C_4H_3 and CH_3. This reaction is exothermic by 138 kJmol^{-1}. However, we could not detect any reactive scattering signal at $m/e=51$ ($C_4H_3^+$) or 50 ($C_4H_2^+$).

B. Laboratory angular distributions (LAB) and TOF spectra

Figures 1–3 display the most probable Newton diagrams of the reaction of atomic carbon with dimethylacetylene and the laboratory angular (LAB) distributions of the C_5H_5 product at collision energies of 21.2, 29.1, and 36.9 kJmol^{-1}. It is

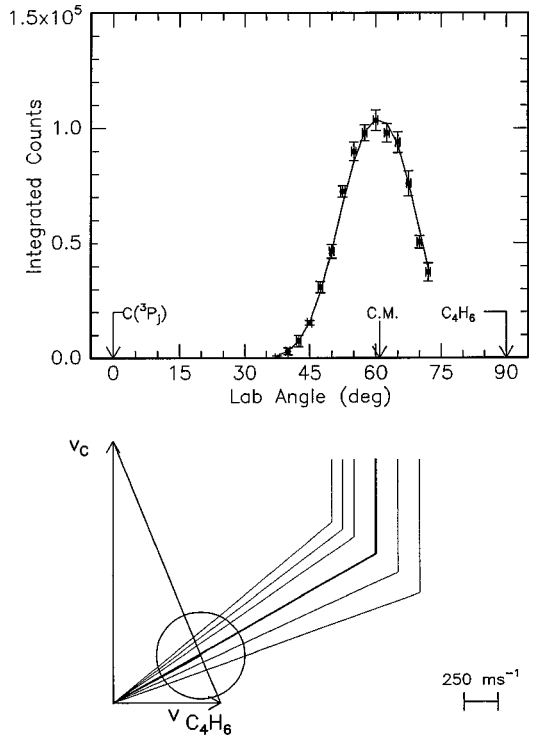

FIG. 1. Lower: Newton diagram for the reaction $C(^3P_j)+CH_3CCCH_3(X^1A_{1g})$ at a collision energy of 21.2 kJmol^{-1}. The circle stands for the maximum center-of-mass recoil velocity of the $H_2CCCCCH_3(X^2A'')$ isomer assuming no energy channels into the internal degrees of freedom. Upper: Laboratory angular distribution of product channel at $m/e=65$. Circles and 1σ error bars indicate experimental data, the solid lines indicate the calculated distribution. C.M. designates the center-of-mass angle. The solid lines originating in the Newton diagram point to distinct laboratory angles whose TOFs are shown in Fig. 4.

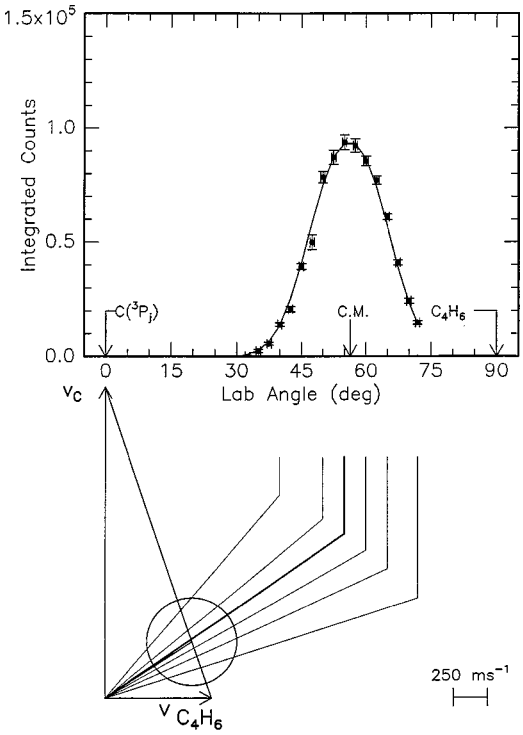

FIG. 2. Lower: Newton diagram for the reaction $C(^3P_j)+CH_3CCCH_3(X^1A_{1g})$ at a collision energy of 29.1 kJmol^{-1}. The circle stands for the maximum center-of-mass recoil velocity of the $H_2CCCCCH_3(X^2A'')$ isomer assuming no energy channels into the internal degrees of freedom. Upper: Laboratory angular distribution of product channel at $m/e=65$. Circles and 1σ error bars indicate experimental data, the solid lines indicate the calculated distribution. C.M. designates the center-of-mass angle. The solid lines originating in the Newton diagram point to distinct laboratory angles whose TOFs are shown in Fig. 5.

evident that at all collision energies, the LAB distribution peaks close to the CM angles, cf. Table I. This finding unravels that the title reaction goes through a complex via indirect reactive scattering dynamics. In addition, all LAB distributions are very broad and extend to about 45.0° in the scattering plane defined by the primary and secondary beams. Together with the C_5H_5+H product mass ratio of 65, these data suggest that the center-of-mass translational energy distributions peak well away from zero. A comparison of the scattering range with the limit circle of the 1-methylbutatrienyl radical assuming all energy channels into the translational degrees of freedom correlates with the signal cut off at 36.5°, 32.5°, and 30.0°. This suggests a significant contribution of this isomer to the reactive scattering signal.

C. Center-of-mass translational energy distributions, $P(E_T)$s

The translational energy distributions $P(E_T)$'s are shown in Figs. 7–9 together with the center-of-mass angular distributions, $T(\theta)$. Best fits of the LAB distributions and TOF data could be achieved with one $P(E_T)$ extending to maximum translational energy releases E_{max} of 190, 210, and 260 kJmol^{-1} from lowest to highest collision energy. Adding or cutting up to 20 kJmol^{-1} in the long energy tail does not change the fit. This high energy cutoff can be employed to identify the product isomer if their energetics are well separated. Here, E_{max} is the sum of the reaction exothermicity plus the relative collision energy. If we subtract the collision energy from the high energy cutoff, we get an experimental exothermicity of 190±25 kJmol^{-1}. Further, all $P(E_T)$'s peak away from zero and have a maxima around 20–30 kJmol^{-1}. This finding suggests that the reaction has a tight exit transition state.

D. Center-of-mass angular distributions, $T(\theta)$, and flux contour maps $I(u,\theta)$

As shown in Figs. 7–9, the shapes of the center-of-mass angular distributions are almost invariant on the collision energy. Best fits of all $T(\theta)$'s are isotropic and symmetric around $\pi/2$. This finding implies that the lifetime of the decomposing C_5H_6 complex(es) is(are) longer than its rotational period τ_r. Alternatively, the decomposing intermediate might have a symmetry axis which can interconvert two H atoms.[17] Here, the light hydrogen atom could be emitted then in θ and θ-π to account for the forward–backward symmetry of $T(\theta)$. Due to the light H atom emission, all our angular distributions are the result of a poor coupling between the initial and final angular momentum vectors, **L** and **L**′, respectively. Due to angular momentum conservation, most of the initial angular momentum channels into rotational excitation of the C_5H_5 product(s).

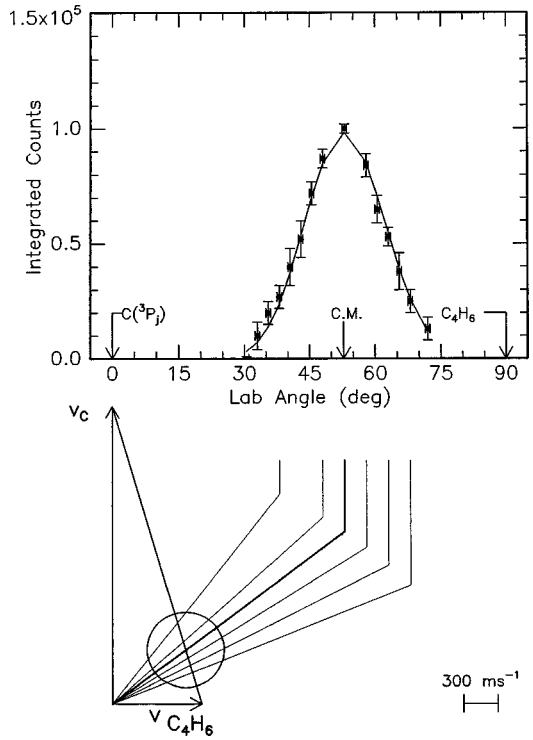

FIG. 3. Lower: Newton diagram for the reaction $C(^3P_j) + CH_3CCCH_3(X^1A_{1g})$ at a collision energy of 36.9 kJmol^{-1}. The circle stands for the maximum center-of-mass recoil velocity of the $H_2CCCCCH_3(X^2A'')$ isomer assuming no energy channels into the internal degrees of freedom. Upper: Laboratory angular distribution of product channel at $m/e=65$. Circles and 1σ error bars indicate experimental data, the solid lines indicate the calculated distribution. C.M. designates the center-of-mass angle. The solid lines originating in the Newton diagram point to distinct laboratory angles whose TOFs are shown in Fig. 6.

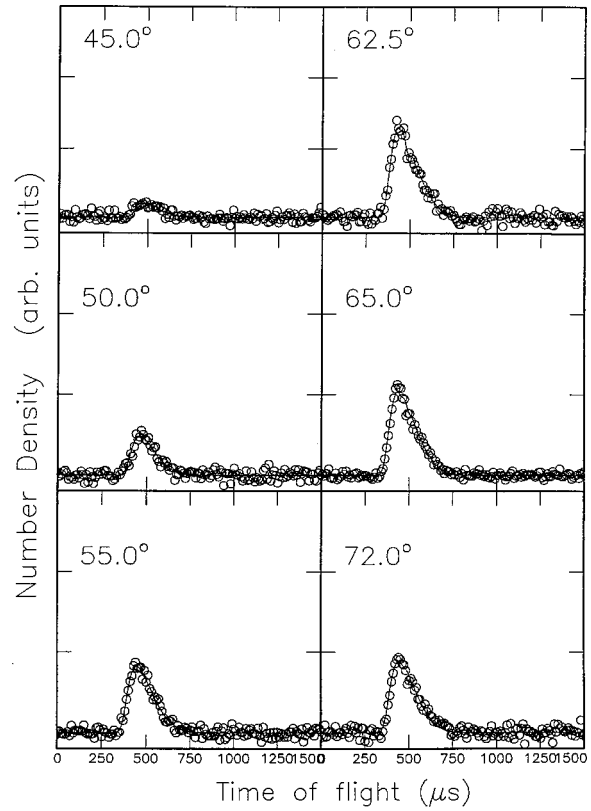

FIG. 4. Time-of-flight data at $m/e=65$ for indicated laboratory angles at a collision energy of 21.2 kJmol^{-1}. Open circles represent experimental data, the solid line represents the fit. TOF spectra have been normalized to the relative intensity at each angle.

Figure 10 shows both two- and three-dimensional center-of-mass flux contour plots $I(\theta,E_T)$ at a selected collision energy of 29.1 kJmol^{-1}. Based on the $T(\theta)$, the best-fit data show a forward–backward symmetric flux profile. Integrating the $I(\theta,E_T)$'s at each collision energy and correcting for the reactant flux as well as relative reactant velocity, we calculate an integrated relative reactive scattering cross section ratio of σ(21.2 kJmol^{-1})/σ(29.1 kJmol^{-1})/σ(36.9 kJmol^{-1})=1.0:0.7±0.1:0.6±0.2 within our error limits. Therefore, the cross section slightly rises as the collision energy decreases. As verified in our electronic structure calculations, cf. Sec. V, this result strongly suggests the reaction proceeds without entrance barrier.

V. DISCUSSION

A. The C_5H_6 potential energy surface

1. Insertion pathway

Despite an extensive investigation, no transition state of a $C(^3P_j)$ insertion into C–H and C–C bonds could be located. We started the saddle point optimization from the geometries with a CCH three-membered ring, suggesting that a C–H bond in dimethylacetylene is broken and two new bonds, C–C and C–H with the attacking carbon atom are formed during the insertion process. This process would lead directly to a $HCCH_2CCCH_3$ intermediate. However, the energies of the initial structures are very high. Upon the transition state search, the C–H bond in dimethylacetylene is restored, and the system descends to the vicinity of **i1**, **i2**, or **i3**, indicating that the insertion pathway does not contain a first-order saddle point. This finding is in strong agreement with previous crossed beam experiments of $C(^3P_j)$ with alkynes, acetylene,[18] and methylacetylene.[19] Therefore, the remaining discussion focuses on the addition of $C(^3P_j)$ to the carbon–carbon triple bond.

2. Addition pathway

The *ab initio* calculations reveal that the dimethylacetylene molecule exists in two conformers (Figs. 11–13). Compared to the eclipsed form, staggered C_4H_6 is more stable by about 0.5 kJmol^{-1}. With the unpaired electrons in the p_x and p_y orbitals, the carbon atom can add without entrance barrier to the π electron density of the carbon–carbon triple bond either to one carbon atom (pathway 1) or two carbon atoms (pathway 2). Pathway 1 can yield triplet trans and cis dimethylpropenediylidene, **i1** and **i2**, respectively. Both isomers have a $^3A''$ electronic wave function and belong to the C_s point group. Here, the trans isomer **i1** is bound by only 132 kJmol^{-1} with respect to the separated reactants; due to the repulsive interaction of both methyl groups, the cis isomer **i2** is 8.0 kJmol^{-1} less stable than the trans form. **i1** and **i2**, however, can isomerize through a transition state located only 10.5 kJmol^{-1} above **i1**. Likewise, **i1** and **i2** can fragment via methyl group loss without exit barrier to **p6**. It is

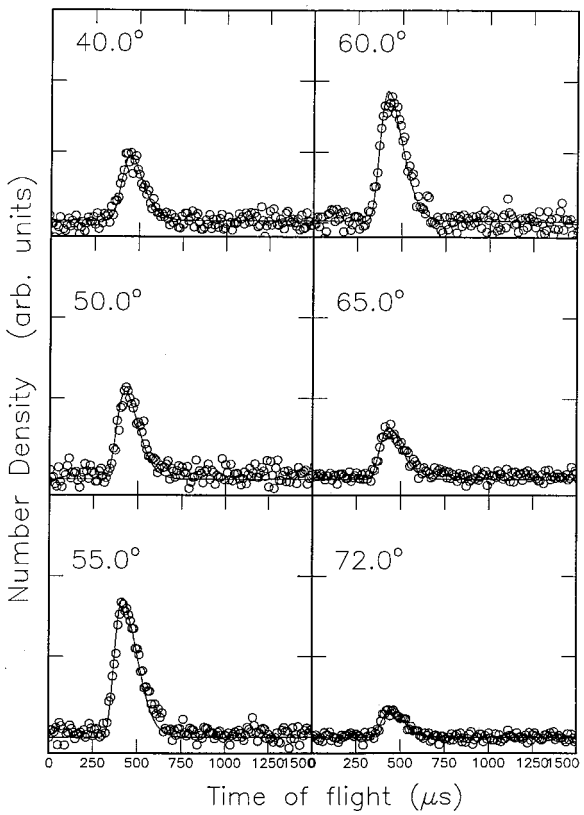

FIG. 5. Time-of-flight data at $m/e=65$ for indicated laboratory angles at a collision energy of 29.1 kJmol^{-1}. Open circles represent experimental data, the solid line represents the fit. TOF spectra have been normalized to the relative intensity at each angle.

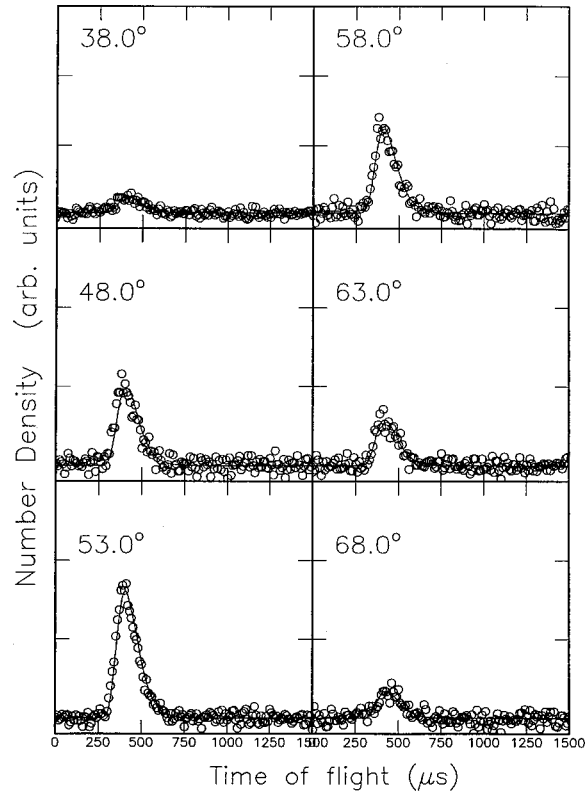

FIG. 6. Time-of-flight data at $m/e=65$ for indicated laboratory angles at a collision energy of 36.9 kJmol^{-1}. Open circles represent experimental data, the solid line represents the fit. TOF spectra have been normalized to the relative intensity at each angle.

worth noting that the newly formed carbon–carbon bonds are 136 pm (**i1**) and 134 pm (**i2**) long; these data lie very close to the carbon–carbon bond in ethylene. Therefore, the new bond can be described as a C═C bond formed by an overlap of the $p_x C(^3P_j)$ orbital with the in-plane π orbital of the C_4H_6 molecule (formation of a C–C σ bond) and of the $p_y C(^3P_j)$ atomic orbital with the out-of-plane π orbital of the dimethylacetylene molecule (formation of a π bond). Further, this process elongates the triple bond in the C_4H_6 molecule from 120 to 140 pm (**i1**) and 137 pm (**i2**); this distance is slightly larger than the double bond in ethylene. Pathway 2 forms the triplet 1,2-dimethylcyclopropenylidene isomer **i3**. The latter has a ^3A electronic wave function, belongs to the C_1 point group, and is energetically favored by 226.0 kJmol^{-1} compared to atomic carbon and dimethylacetylene. If we compare the bond distances in **i3** with those in the reactants, it is evident that the former carbon–carbon triple bond is elongated from 120 to 158 pm; this data is very characteristic of a C–C bond such as in the ethane molecule (154 pm). In addition, the newly formed bonds are 130 and 143 pm long, close to an olefinic bond of 134 pm as found in ethylene. An alternative route to **i3** goes via ring closure of **i2**: here, triplet dimethylpropenediylidene is metastable and only separated by a barrier of 1.5 kJmol^{-1} from **i3**.

i3 can either isomerize or react to the products. First, a [1,2]-H shift via a barrier of 210 kJmol^{-1} can form the chain isomer **i5** ($^3A,C_1$). The latter can be rationalized as a triplet methylvinylvinylidene carbene which is 45.0 kJmol^{-1} less stable than **i3**. A second pathway is the ring opening via a 65.0 kJmol^{-1} barrier of **i3** to the linear isomer triplet dimethylpropargylene **i4**. **i4** belongs to the D_{3d} point group, has a ^3E_g electronic wave function, and is stabilized by 375.0 kJmol^{-1} with respect to the reactants. The carbon–carbon distances in the propargylene unit are 127 pm and therefore between those of a triple bond (120 pm) and a double bond (134 pm). Compared to **i4**, the unsubstituted triplet propargylene, 1-HCCCH, has C_2 symmetry. The different point groups could be rationalized as follows: replacing both hydrogen atoms by a methyl group results in an increased repulsion of both CH_3 units; a change to a linear geometry maximizes the distance of both methyl groups and hence minimized the energy. A carbon–hydrogen bond rupture in **i4** via a tight transition state located 18.0 kJmol^{-1} above the products leads finally to the 1-methylbutatrienyl isomer **p1**, CH_3CCCCH in its $^2A''$ electronic ground state. The exothermicity from the products to **p1**+H is calculated to be 180.0 kJmol^{-1}. Compared to **p1**, the unsubstituted C_4H_3 isomer H_2CCCCH is bent; its linear structure is only a transition state. In strong analogy to the (dimethyl)propargylene isomers, substituting a H atom by a CH_3 in C_4H_3 favors the linear geometry as well. In addition, a methyl loss in **i4** can yield the linear CH_3CCC isomer (**p6**) without exit barrier. Compared to the cyclic isomer, the linear structure is more stable by 25.0 kJmol^{-1}. We like to point out that in strong contrast to the unsubstituted C_3H isomers (the cyclic isomer is more stable by 7.0 kJmol^{-1})[20] the stability of the methyl

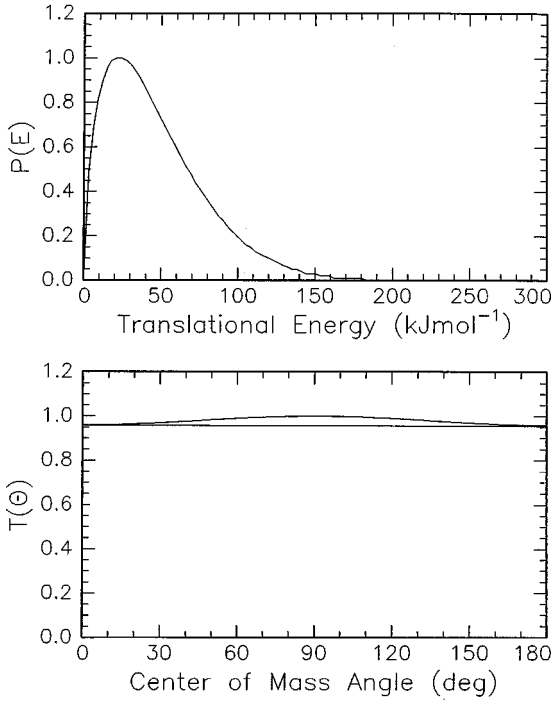

FIG. 7. Lower: Center-of-mass angular flux distributions for the reaction $C(^3P_j)+CH_3CCCH_3(X^1A_{1g})$ at a collision energy of 21.2 kJmol^{-1}. Upper: Center-of-mass translational energies flux distribution for the reaction $C(^3P_j)+CH_3CCCH_3(X^1A_{1g})$ at a collision energy of 21.2 kJmol^{-1}.

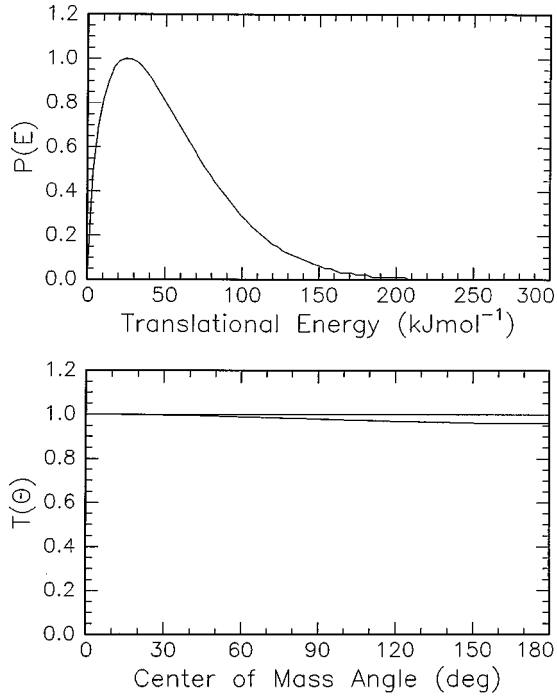

FIG. 8. Lower: Center-of-mass angular flux distributions for the reaction $C(^3P_j)+CH_3CCCH_3(X^1A_{1g})$ at a collision energy of 29.1 kJmol^{-1}. Upper: Center-of-mass translational energies flux distribution for the reaction $C(^3P_j)+CH_3CCCH_3(X^1A_{1g})$ at a collision energy of 29.1 kJmol^{-1}.

substituted forms **p6** and **p7** are reversed, and the linear form is more stable than the cyclic isomer. Alternatively, **i3** can decompose via C–H or C–CH_3 bond ruptures through tight exit transition states located 10.0 and 14.0 kJmol^{-1} above **p4**+H and **p6**+CH_3. The overall reactions from $C(^3P_j)$ and dimethylacetylene are exothermic by 67.7 and 62.0 kJmol^{-1}, respectively.

The fate of **i5** is governed by a H atom shift together with ring closure via a barrier of 175.0 kJmol^{-1} to **i6**. The latter can decompose via three distinct H atom loss channels to the cyclic C_5H_5 isomers **p2**, **p4**, or **p5**. All isomers are energetically less favorable than the most stable 1-methylbutatrienyl radical **p1** by 23.5, 110, and 114 kJmol^{-1}. Alternatively, **i6** undergoes H atom migration (190 kJmol^{-1} barrier) to **i7**. The later can be described as an allyl-substituted vinyl isomer. It resides in a deep potential energy well of 390 kJmol^{-1} with respect to the reactants and is the global minimum on this part of the triplet C_5H_6 potential energy surface. **i7** can undergo another H shift (178 kJmol^{-1} barrier) to form **i8** which fragments to **p2** or **p3**. We would like to point out that all barriers for a H atom migration lie in a very narrow range between 170 and 210 kJmol^{-1}. The transition states for these hydrogen splittings have all late character with C–H distances between 190 and 230 pm.

Finally, we would like to stress that since barriers of H atom migrations are typically within 170 to 200 kJmol^{-1}, a methyl group migration in **i1** and **i2** is expected to involve an even higher barrier. Because this barrier lies well above the collision energy of our experiments, the formation of triplet dimethylvinylidene-carbene, $CCC(CH_3)_2$, or **i4** via methyl group shift can be eliminated from the following discussion.

B. Identification of reaction product(s)

Our translational energy distributions, $P(E_T)$'s, suggest that the formation of the C_5H_5 isomer(s) is exothermic by 190±25 kJmol^{-1}. A comparison of these data with the cal-

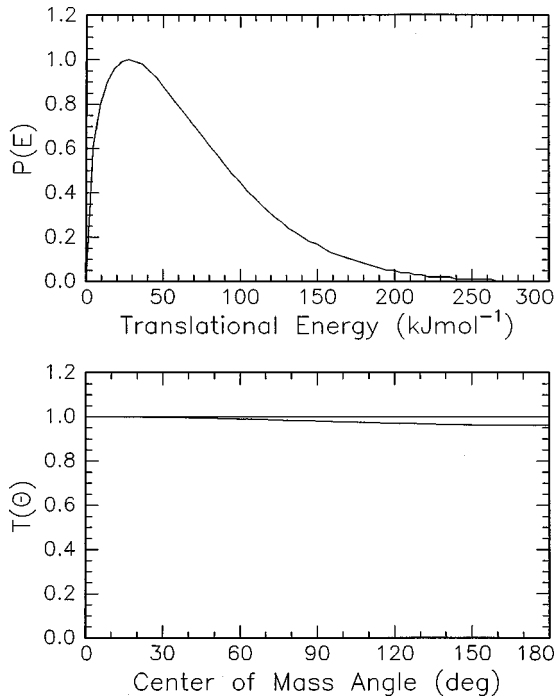

FIG. 9. Lower: Center-of-mass angular flux distributions for the reaction $C(^3P_j)+CH_3CCCH_3(X^1A_{1g})$ at a collision energy of 36.9 kJmol^{-1}. Upper: Center-of-mass translational energies flux distribution for the reaction $C(^3P_j)+CH_3CCCH_3(X^1A_{1g})$ at a collision energy of 36.9 kJmol^{-1}.

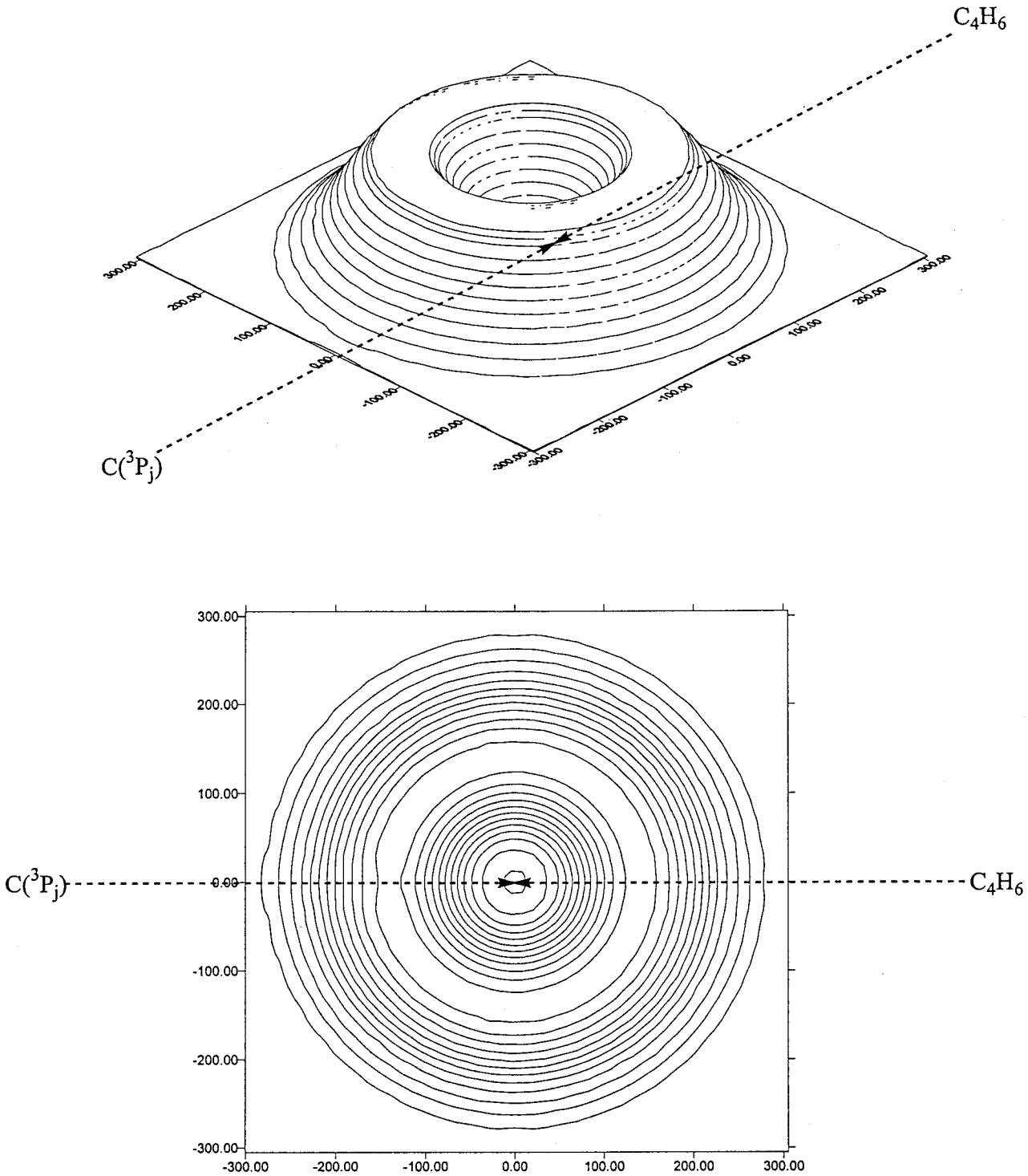

FIG. 10. Contour flux map for the reaction $C(^3P_j)+CH_3CCCH_3(X^1A_{1g})$ at a collision energy of 29.1 kJmol^{-1}. (a) Three-dimensional map and (b) two-dimensional projection. Units are given in ms^{-1}.

culated reaction energies reveals that at least the thermodynamically most stable C_5H_5 isomer, 1-methylbutatrienyl (**p1**), is formed. The calculated data of 180.0 kJmol^{-1} is in excellent agreement with our experimental value. This finding is strongly supported by the potential energy surface and our RRKM calculations. Here, **p1** can only be synthesized via the reaction sequence **i3**→**i4**→**p1**+H. As discussed in the previous section, alternative reaction pathways of **i3** involve significant barriers which are energetically less favorable by at least 110 kJmol^{-1} compared to the ring opening of **i3** to **i4**. As verified in our RRKM calculations, the rate constant of the **i3**→**i4** isomerization is found to be about three to four orders of magnitude larger than those of **i3**→**i5**, **i3**→**p6**+CH_3, and **i3**→**p4**+H. Therefore, we must conclude that the 1-methylbutatrienyl radical is the sole reaction product, and the contribution of **p2**–**p8** is minimal.

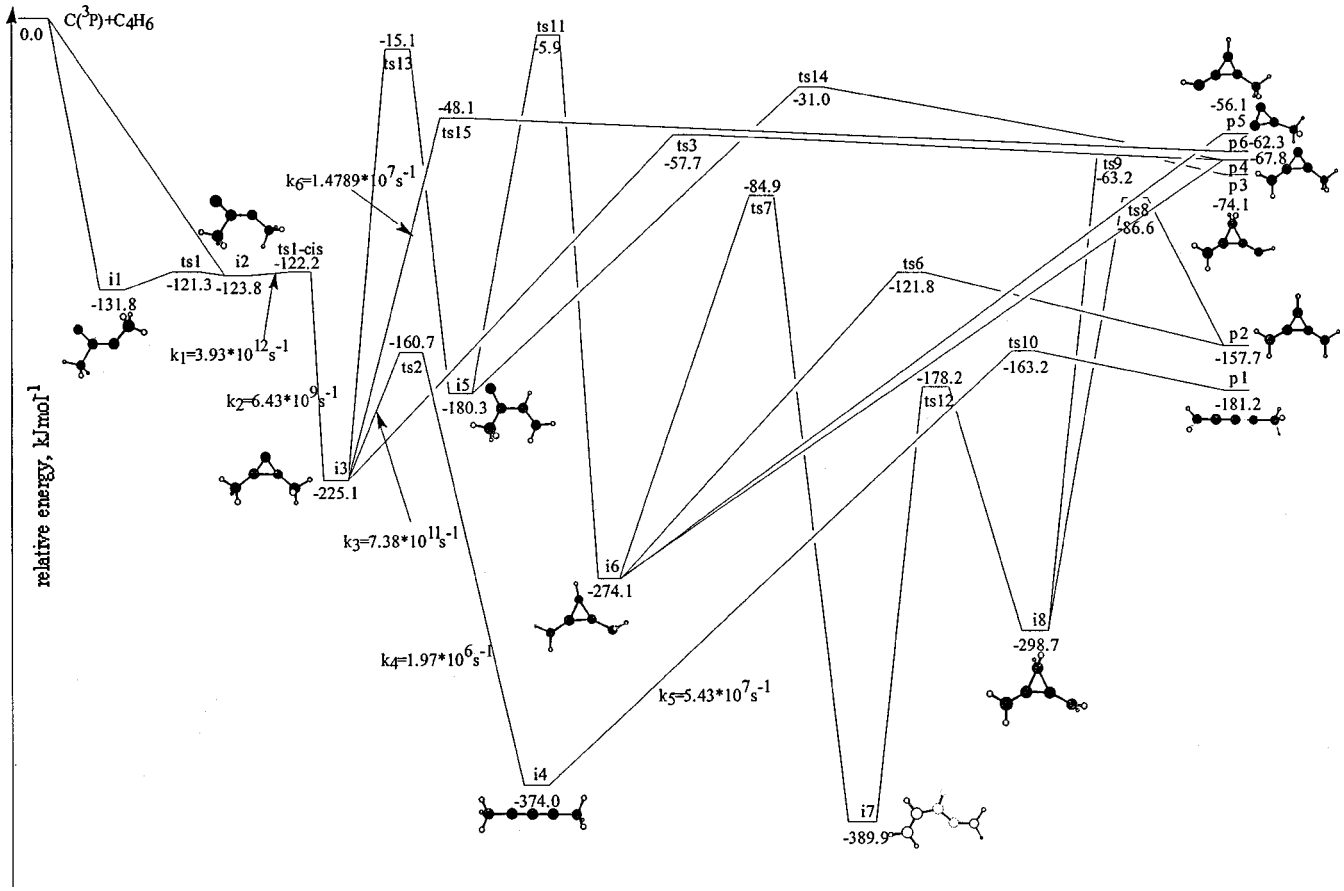

FIG. 11. Schematic representation of the lowest energy pathways on the triplet C_5H_6 PES. Those structures designated with ''*i*'' indicate intermediates, those with ''*p*'' potential C_5H_5 isomers. RRKM calculated rate constants for individual reaction steps are also shown.

C. The actual reaction pathway on the C_5H_6 potential energy surface

The reaction dynamics to form the 1-methylbutatrienyl radical, $H_2CCCCCH_3(X^2A'')$, are governed by indirect scattering dynamics and proceed via a barrierless addition of $C(^3P_j)$ to the carbon–carbon triple bond of the dimethylacetylene molecule. Here, the p_x and p_y orbitals of $C(^3P_j)$ can interact with the π electron density of the triple bond to form **i1**/**i2** (sideways attack) or **i3** (almost perpendicular attack to the carbon–carbon triple bond). Since the barrier of trans-cis isomerization of **i1**/**i2** lies well below the total available energy, this process is very rapid; therefore both isomers are expected to exist in equal amounts. Due to the steric effect of the bulky methyl groups, it is very likely that the approaching carbon atom reacts preferentially on the ^3A surface to **i3**. This pathway supports a maximum orbital overlap to form two C–C–σ bonds in triplet dimethylcyclopropenylidene. Although we cannot quantify the formation of the initial collision complexes **i1**/**i2** versus **i3** at the present stage, the RRKM calculations show that the **i2** to **i3** conversion is very fast ($k=7\times10^9\ s^{-1}$). Therefore, all initially formed **i1**/**i2** complexes undergo ring closure to **i3**. The latter ring opens to form the triplet dimethylpropargylene isomer **i4**. Since the dimethylacetylene molecules are prepared in a supersonic expansion, their rotational angular momentum is negligible. Hence in a good approximation the total angular momentum **J** is the initial orbital angular momentum **L**.

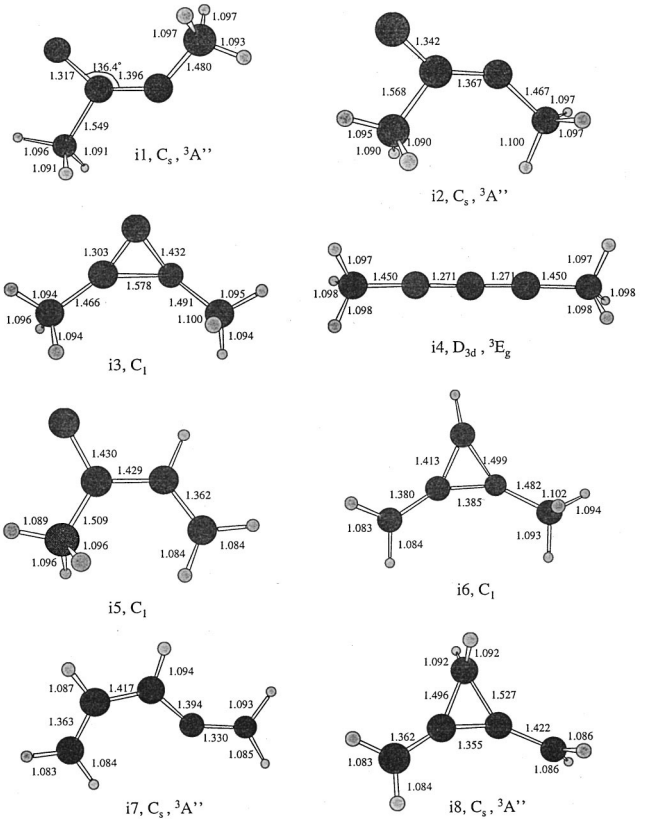

FIG. 12. Structures of potentially involved triplet C_5H_6 collision complexes. Bond lengths are given in Angstrom, bond angles in degrees.

Since $\mathbf{L}\approx\mathbf{J}$, the highly prolate **i4** (asymmetry parameter $\kappa=-0.999$) rotates around its C_2 symmetry axis almost parallel to the total angular momentum vector **J**. Employing the symmetric top approximation as outlined in Ref. 21, we find that rotations of **i4** around the C_3 symmetry axis, i.e., the internuclear axis on which all carbon atoms are arranged, are energetically not accessible. Finally, **i4** decomposes via H emission through a tight transition state located 18.0 kJmol^{-1} above the products to the experimentally observed 1-methylbutatrienyl radical. The finding of a tight exit transition state are reflected in our electronic structure calculations as well showing an imaginary frequency of 692*i* cm^{-1}. Likewise, this finding correlates with the center-of-mass translational energy distributions depicting distribution maxima at 20–30 kJmol^{-1}. Further, the *ab initio* exit barrier of 18.0 kJmol^{-1} corresponds closely to typical barriers of H atom addition to double or triple bonds.

The decomposing triplet dimethylpropargylene complex **i4** is very interesting. First, it resides in a deep potential energy well of 375.0 kJmol^{-1}. This finding could explain the experimentally observed forward–backward symmetric center-of-mass angular distributions, cf. Figs. 7–9, and the fragmenting complex has a lifetime longer than its rotation period. Second, **i4** rotates around its C_2 axis, and can therefore interconvert the leaving hydrogen atom, cf. Sec. IV D. Therefore, the isotropic $T(\theta)$'s could be the result of the symmetric reaction intermediate as well, and we cannot gain information on the lifetime of **i4**. If we compare our findings with the reaction of atomic carbon and 1,3-butadiene, we find that the decomposing C_5H_6 complex resides in a similar deep potential energy well of 360 kJmol^{-1}. Since both reactions have a similar exothermicity and the forward–backward symmetric center-of-mass angular distributions were found in this reaction as well, we suggest that our title reaction proceeds through a long-lived complex **i4**. These indirect scattering dynamics are supported by the average fraction of total available energy of 30% channeling into the translational degrees of freedom of the 1-methylbutatrienyl radical and H atom. This data is similar to a value of 30% to 35% as found in the reaction of atomic carbon with 1,3-butadiene.

D. Comparison with the reaction of $C(^3P_j)$ with 1,3-butadiene

The reactions of atomic carbon with both C_4H_6 isomers dimethylacetylene and 1,3-butadiene have no entrance barrier and depict a similar energy dependence of the integrated relative reactive cross sections σ. Here, σ decreases slightly as the collision energy increases, i.e., σ(21.2 kJmol^{-1})/σ(29.1 kJmol^{-1})/σ(36.9 kJmol^{-1})=1.0:0.7 $\pm$0.1:0.6$\pm$0.2 (dimethylacetylene) and σ(19.3 kJmol^{-1})/σ(28.0 kJmol^{-1})/σ(38.8 kJmol^{-1})=1.0:0.7$\pm$0.2:0.5$\pm$0.1 (1,3-butadiene). These findings together with recent kinetic data[22] suggest that both reactions are dominated by attractive long-range dispersion forces. Further, all reactions proceed via addition of $C(^3P_j)$ to the π electronic system of the unsaturated hydrocarbon; no insertion into C–H or C–C single bonds could be observed. In addition, both reactions are governed by indirect scattering dynamics and about 25% to 35% of the total available energy channels into the translational degrees of freedom of the products. The decomposing complexes reside in deep potential energy wells of 375.0 kJmol^{-1} (dimethylacetylene) and 330.0 kJmol^{-1} (1,3-butadiene) and fragment via C–H bond rupture through tight transition states located about 20 kJmol^{-1} above the products. This carbon versus hydrogen exchange is the dominant process. The methyl (dimethylacetylene) loss channel was not observed. Here, the methyl radical can be formed from **i3** or **i4**. The CH_3 loss in **i3** occurs with an exit barrier of 14 kJmol^{-1} and the total exothermicity of the $C(^3P_j)+H_3CCCCH_3\rightarrow CH_3+c\text{-}CCCCH_3$ reaction is 62 kJmol^{-1}. However, the calculated rate constant for the **i3**→**i4** isomerization, $7.4\times10^{11}\,s^{-1}$, is about 50 000 times higher than that for the CH_3 loss, making this channel very unlikely. A linear $CCCCH_3$ could be produced by the CH_3 lost from **i4**. In this case, the reaction does not have an exit barrier but the overall reaction exothermicity is even lower, 36.7 kJmol^{-1}. From the comparison of the barrier heights for the hydrogen elimination in **i4**, 211 kJmol^{-1}, and for CH_3 elimination in **i4**, 337 kJmol^{-1}, we can conclude that the latter reaction channel is not expected to compete with the former.

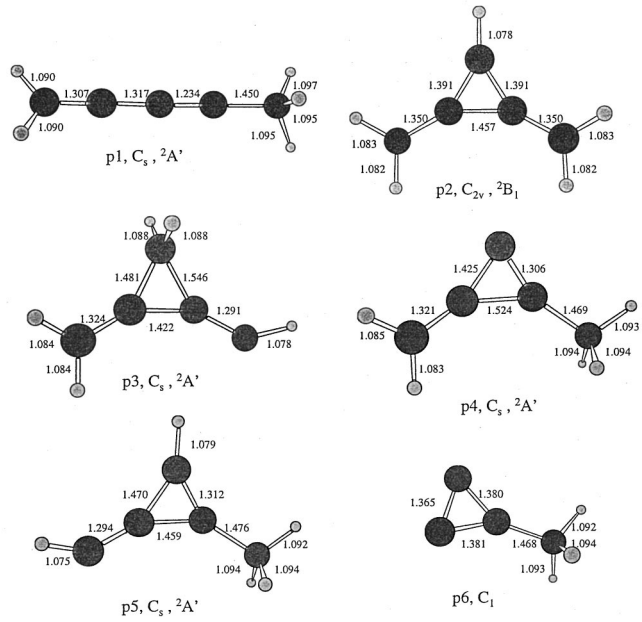

FIG. 13. Structures of doublet C_5H_5 isomers. Bond lengths are given in Angstrom, bond angles in degrees.

Despite these similarities, both systems show striking differences. Whereas the reaction of $C(^3P_j)$ with 1,3-butadiene forms 1- and 3-vinylpropargyl radicals, $HCCCH-C_2H_3(X^2A'')$, and $H_2CCC-C_2H_3(X^2A'')$, the title reaction gives the 1-methylbutatrienyl radical, $H_2CCCCCH_3(X^2A'')$. This is a direct consequence of the involved potential energy surfaces. In strong contrast to the $C(^3P_j)/CH_3CCH$ (Ref. 19) and $C(^3P_j)/H_2CCCH_2$ (Ref. 23) systems, which both form the thermodynamically most stable n-C_4H_3 isomer, the PESs of $C(^3P_j)/C_2H_3C_2H_3$ and $C(^3P_j)/CH_3CCCH_3$ are only coupled via **i6**, cf. Fig. 14. A [2,1]-H atom migration in the long-lived triplet vinylallene complex as formed in the reaction of $C(^3P_j)$ with 1,3-

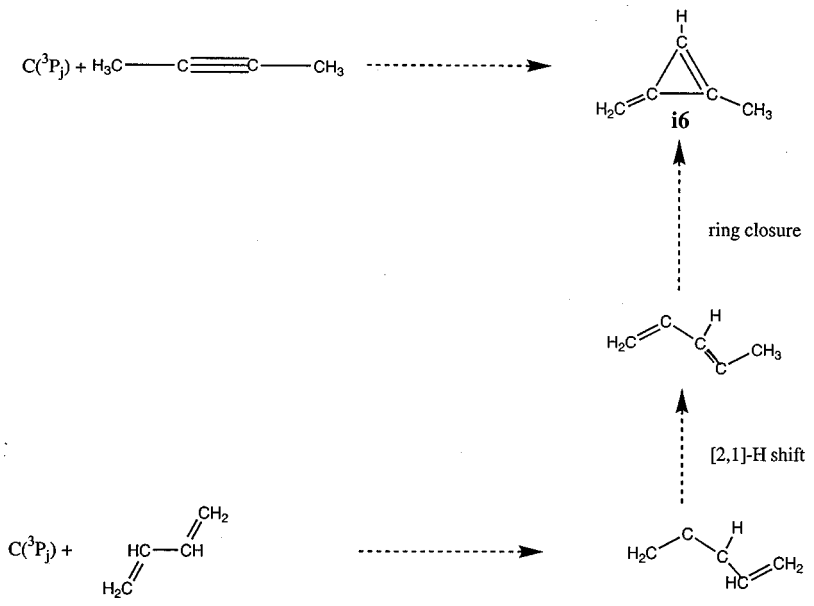

FIG. 14. Schematic representation of the coupling of the $C(^3P_j)/CH_3CCCH_3$ and the $C(^3P_j)/C_2H_3C_2H_3$ potential energy surfaces.

butadiene results in a triplet diradical which can undergo ring closure to **i6**. Due to the expected H atom migration barrier of about 200 $kJmol^{-1}$, this pathway plays no role in our crossed beam experiments, but might be significant in high-temperature combustion flames.

We would like to stress, however, that although the product isomers are different in both reactions and the chemical reaction dynamics involve distinct intermediates, in denser reaction media such as combustion flames and outflow of carbon rich stars 3-vinylpropargyl, $H_2CCC–C_2H_3$, can isomerize via a [1,2] hydrogen shift to 1-methylbutatrienyl radical, $H_2CCCCCH_3$, cf. Fig. 15. Likewise a H atom addition to the terminal carbon atom in 3-vinylpropargyl to $H_2CCC–CHCH_3$ followed by an H atom elimination at C2 leads to the 1-methylbutatrienyl isomer. Since a H atom shift is expected to have a barrier of about 200 $kJmol^{-1}$, but a H atom addition/elimination only involve barriers of about 15–25 $kJmol^{-1}$, the two-step addition-elimination pathway should dominate the isomerization. The energetics of these processes are currently under investigation.

E. Comparison of the reactions of $C(^3P_j)$ with acetylene and methylacetylene

The involved potential energy surfaces and chemical dynamics of $C(^3P_j)$ reactions with (methyl-substituted) acetylene show strong similarities. First, reactions with acetylene, methylacetylene, and dimethylacetylene are governed by indirect scattering dynamics via complex formation; 30%–35% of the total available energy channels into the translational degrees of freedom. $C(^3P_j)$ attacks the carbon–carbon triple bond without entrance barrier to either one or both carbon atoms. These pathways yield (substituted) propendiylidene and/or (substituted) cyclopropenylidene intermediates which are stabilized by 124–137 $kJmol^{-1}$ and 216–227 $kJmol^{-1}$ with respect to the reactants, cf. Table II. The propenediylidene and methylpropenediylidene isomers undergo H atom migration to form (methyl)propargylene radicals. All (substituted)cyclopropenylidene intermediates can show a ring opening to (substituted)propargylene radicals via barriers between 55 $kJmol^{-1}$ and 60 $kJmol^{-1}$. These intermediates are in deep potential energy wells of 374–388

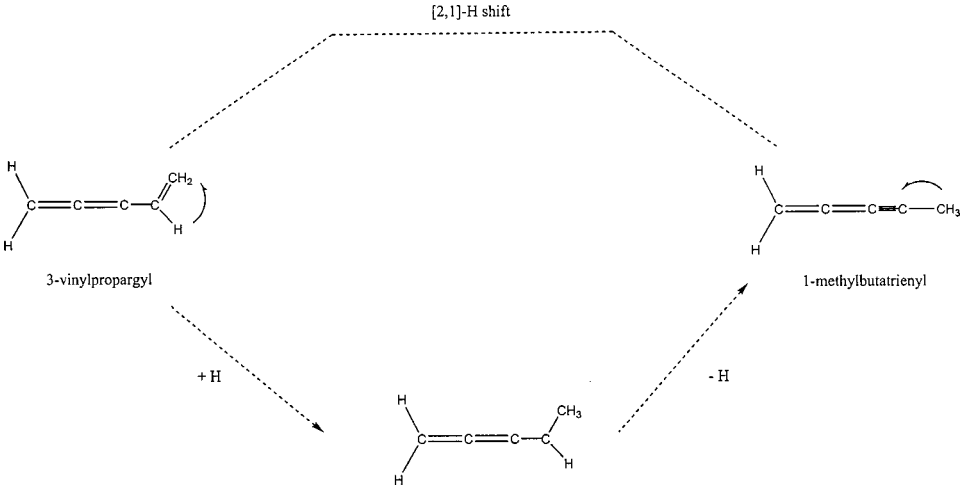

FIG. 15. Schematic representation of the isomerization of 3-vinylpropargyl, $H_2CCC-C_2H_3$, to the 1-methylbutatrienyl radical, $H_2CCCCCH_3$.

TABLE II. Comparison of intermediates, energetics, symmetries, and electronic wave functions in reactions of atomic carbon with (substituted) acetylenes. All energies are given with respect to the separated reactants.

Isomer	Electronic wave function	Point group	Energy kJmol^{-1}	Electronic wave function	Point group	Energy, kJmol^{-1}	Electronic wave function	Point group	Energy, kJmol^{-1}
	$R=H$; $R'=H$ acetylene[a]			$R=H$; $R'=CH_3$ methylacetylene[b]			$R=CH_3$; $R'=CH_3$ dimethylacetylene[c]		
CRCCR′ (trans) propenediylidene	A''	C_s	−137	A''	C_s	−137	A''	C_s	−132
CRCCR′ (cis) propenediylidene	a	a	a	A''	C_s	−136	A''	C_s	−124
c-RC3R′ cyclopropenylidene	A	C_1	−216	A	C_1	−221	A	C_1	−227
RCCCR′ propargylene	B	C_2	−388	A	C_1	−374	E_g	D_{3d}	−375
CCCRR′ vinylidenecarbene	B_1	C_{2v}	−253	A''	C_s	−223	A''	C_s	−242

[a]The cis isomer was found not to be a local minimum; see References 18, 20, and 25.
[b]Reference 19.
[c]Present work.

kJmol^{-1} and decompose via H atom loss; no CH_3 loss was observed. Finally, the reaction exothermicities to form the n-C_4H_3 isomer and the 1-methylbutatrienyl radical are very similar and are calculated to be around 180 kJmol^{-1}.

VI. CONCLUSIONS

The reaction of ground state carbon atoms, $C(^3P_j)$, with dimethylacetylene, H_3CCCCH_3, was studied at three collision energies between 21.2 and 36.9 kJmol^{-1} employing the crossed molecular beam technique. Our experiments were combined with *ab initio* and RRKM calculation. It is found that the reaction is barrierless via a loose, early transition state located at the centrifugal barrier and follows indirect scattering dynamics through a complex. This process forms a dimethylcyclopropeneylidene intermediate either in one step via an addition of $C(^3P_j)$ to C1 and C2 of the acetylenic bond or through an addition to only one carbon atom to short-lived cis/trans dimethylpropendiylidene intermediates followed by ring closure. The cyclic intermediate ring opens to a linear dimethylpropargylene. This complex fragments to atomic hydrogen and a linear 1-methylbutatrienyl radical, $H_2CCCCCH_3(X^2A'')$, via a tight exit transition state located 18.0 kJmol^{-1} above the separated products. The experimentally determined exothermicity of 190±25 kJmol^{-1} is in strong agreement with our calculated data of 180±10 kJmol^{-1}. The explicit verification of the carbon versus hydrogen exchange pathway together with the first identification of the $H_2CCCCCH_3$ radical represents a third pathway to form chain C_5H_5 radicals in the reactions of $C(^3P_j)$ with C_4H_6 isomers under single-collision conditions. Previous experiments of atomic carbon with the 1,3-butadiene isomer verified the formation of 1- and 3-vinylpropargyl radicals, $HCCCH–C_2H_3(X^2A'')$, and $H_2CCC–C_2H_3(X^2A'')$, respectively. In high-density environments such as combustion flames and circumstellar envelopes of carbon stars, these linear isomers can undergo collision-induced ring closure(s) and/or H atom migration(s) which can lead to the cyclopentadienyl radical. The latter is thought to be a crucial reactive intermediate in soot formation and possibly in the production of polycyclic aromatic hydrocarbon molecules in outflow of carbon stars.

ACKNOWLEDGMENTS

R.I.K. is indebted the Deutsche Forschungsgemeinschaft for a *Habilitation* fellowship (IIC1-Ka1081/3-1). This work was supported by Academia Sinica, Taiwan, the National Science Council of R.O.C., and by the Petroleum Research Fund of R.O.C. This work was performed within the international astrophysics network (http://po.iams.sinica.edu.tw/~kaiser/network.htm).

[1] N. M. Marinov *et al.*, Combust. Flame **114**, 192 (1998); N. M. Marinov *et al.*, Combust. Sci. Technol. **116/117**, 211 (1996); N. M. Marinov *et al.*, *ibid.* **128**, 295 (1997).
[2] C. Melius *et al.*, *Twenty-sixth Symposium on Combustion/The Combustion Institute* (1996), p. 685.
[3] H. W. Jochims, E. Rühl, H. Baumgärtel, S. Tobita, and S. Leach, Astrophys. J. **420**, 307 (1994); P. Ehrenfreund, B. H. Foing, L. d'Hendecourt, P. Jeniskens, and F. X. Desert, Astron. Astrophys. **299**, 213 (1999); M. Frenklach and E. D. Feigelson, Astrophys. J. **341**, 372 (1998); G. von Helden, N. G. Gotts, and M. T. Bowers, Nature (London) **363**, 60 (1993); J. M. Hunter, J. L. Fye, E. J. Roskamp, and M. F. Jarrold, J. Phys. Chem. **98**, 1810 (1994).
[4] N. M. Marinov *et al.*, Combust. Sci. Technol. **128**, 295 (1997).
[5] M. J. Castaldi *et al.*, *Twenty-sixth Symposium on Combustion/The Combustion Institute* (1996), p. 693.
[6] I. Hahndorf, H. Y. Lee, A. M. Mebel, Y. T. Lee, and R. I. Kaiser, J. Chem. Phys. **113**, 9622 (2000), preceding paper.
[7] Y. T. Lee, J. D. McDonald, P. R. LeBreton, and D. R. Herschbach, Rev. Sci. Instrum. **40**, 1402 (1969).
[8] R. I. Kaiser and A. G. Suits, Rev. Sci. Instrum. **66**, 5405 (1995).
[9] G. O. Brink, Rev. Sci. Instrum. **37**, 857 (1966).
[10] M. S. Weis, Ph.D. thesis, University of California, Berkeley, 1986; M. Vernon, thesis, University of California, Berkeley, 1981.
[11] A. D. Becke, J. Chem. Phys. **98**, 5648 (1993); C. Lee, W. Yang, and R. G. Parr, Phys. Rev. B **37**, 785 (1988).
[12] R. Krishnan, M. Frisch, and J. A. Pople, J. Chem. Phys. **72**, 4244 (1980).
[13] A. M. Mebel, K. Morokuma, and M. C. Lin, J. Chem. Phys. **103**, 7414 (1995).
[14] GAUSSIAN 98, Revision A.7, M. J. Frisch, G. W. Trucks, H. B. Schlegel *et al.* (Gaussian, Inc., Pittsburgh, PA, 1998).
[15] MOLPRO is a package of *ab initio* programs written by H.-J. Werner and P.

J. Knowles, with contributions from J. Almlöf, R. D. Amos, M. J. O. Deegan, S. T. Elbert, C. Hampel, W. Meyer, K. Peterson, R. Pitzer, A. J. Stone, P. R. Taylor, and R. Lindh.
[16] H. Eyring, S. H. Lin, and S. M. Lin, *Basis Chemical Kinetics* (Wiley, New York, 1980).
[17] W. B. Miller, S. A. Safron, and D. R. Herschbach, Discuss. Faraday Soc. **44**, 108,291 (1967); W. B. Miller, Ph.D. thesis, Harvard University, Cambridge, 1969.
[18] R. I. Kaiser, C. Ochsenfeld, M. Head-Gordon, Y. T. Lee, and A. G. Suits, Science **274**, 1508 (1996).
[19] R. I. Kaiser, D. Stranges, Y. T. Lee, and A. G. Suits, J. Chem. Phys. **105**, 8721 (1996); A. M. Mebel, R. I. Kaiser, and Y. T. Lee, J. Am. Chem. Soc. **122**, 1776 (2000).
[20] C. Ochsenfeld, R. I. Kaiser, A. G. Suits, Y. T. Lee, and M. Head-Gordon, J. Chem. Phys. **106**, 4141 (1997).
[21] R. I. Kaiser, Y. T. Lee, and A. G. Suits, J. Chem. Phys. **105**, 8705 (1996).
[22] D. C. Clary, N. Haider, D. Husain, and M. Kabir, Ap. **422**, 416 (1994).
[23] R. I. Kaiser, A. M. Mebel, A. H. H. Chang, S. H. Lin, and Y. T. Lee, J. Chem. Phys. **110**, 10330 (1999).
[24] G. Scoles, *Atomic and Molecular Beam Data* (Oxford U.P., Oxford, 1992).
[25] R. I. Kaiser, C. Ochsenfeld, M. Head-Gordon, Y. T. Lee, and A. G. Suits, J. Chem. Phys. **106**, 1729 (1997).